INDUCED SICKLING OF ERYTHROCYTES VIA BENDING AND THE EFFECT OF MECHANICAL PROPERTIES ON CELL PORE ENTRY

A Thesis presented to the Department of

Materials Science and Engineering

African University of Science and Technology, Abuja

In Partial Fulfillment of the Requirements

For the Degree of

MASTER OF SCIENCE

BY

UZONWANNE, VANESSA OBIAGELI

DECEMBER, 2014

SIGNATURE PAGE

ABSTRACT

Patients living with sickle cell disease are perpetually plagued with painful crisis episodes, caused by vascular occlusion. Over time, this leads to oxygen deprivation and the eventual damage of starved tissues and organs. Observations stemming from mechanical characterization of both diseased and healthy red blood cells (RBC), establish that shape and mechanical properties of human red blood cells are essential in maintaining normal functionality of these cells. From a molecular biology stand point the sickling process has been mapped out yet there is a gap in the actual mode of deformation that results in the characteristic sickle or crescent shape observed experimentally. As a consequence, this research proposes that bending forces imposed by internal RBC structures are a possible culprit and utilizes Abaqus™ software to model the sickling of an erythrocyte with sickle cell traits under bending conditions. Critical Pressure value required for cell pore aspiration of a normal erythrocyte, oxygenated and deoxygenated sickle cell are also estimated for their respective moduli. It was found that bending could cause morphological sickling but the model did not account for change in modulus upon deformation. Critical Pressure value increased from normal, to oxygenated and then to deoxygenated sickle cell which tally's with the trend in decreasing Aspiration ratio calculated.

ACKNOWLEDGEMENT

This work was made possible by the grace of the Almighty God and the support of various people I am grateful to.

First my appreciation goes to my supervisor, Prof. W. O. Soboyejo for his guidance, encouragement and push to get this work done. I appreciate his positive criticisms and input to making this work what it has become.

To Mr. Chukwu Emeka Ani and Joseph Asare for being there to guide me in the use of the Abaqus™ software, for the tireless hours they put into brain storming with me, I am forever grateful for all their help and for also introducing me to the mendely referencing software.

To Mr. Emmanuel Arthur for teaching me the rudiments of bending and for guiding me through my analytical model.

To Mr. Danyuo Yiporo for teaching me how to use the origin soft ware which was helpful throughout this work.

To the AUST chapter of African Materials Society members, for their constructive criticism during our weekly seminar meetings, the wealth of knowledge gained was priceless.

To my fellow M.Sc colleagues at the Materials Science and Engineering Department, I am glad to have shared this space and time with you. To the African Development Bank, AUST community I am grateful for the opportunity given to me to broaden my knowledge. I say thank you to you all.

DEDICATION

This Thesis Is Dedicated to God, The Pillar and Reason for my Being.

To My Family for their Love, Care and constant support,

and to My Brothers and Sisters in the Lord for their Ceaseless Prayers and Understanding.

TABLE OF CONTENTS

SIGNATURE PAGE i

ABSTRACT ii

ACKNOWLEDGEMENT iii

DEDICATION iv

TABLE OF CONTENTS v

LIST OF FIGURES viii

LIST OF TABLES ix

Chapter 1 1

1.0 INTRODUCTION 1

1.1 Background and Motivation 1

1.2 Research Objectives 2

1.3 Scope of Research 2

1.4 Outline of Thesis 3

Chapter 2 4

2.0 LITERATURE REVIEW 4

2.1 Introduction 4

2.2 The Red Blood Cell (RBC, Erythrocyte) 5

2.2.1 Function of Erythrocyte membrane 5

2.2.1.1 Deformability of the RBC Membrane 5

2.3 Sickle Cell Disease 6

2.4 Common Experimental Approaches to Mechanical Characterization of Cells 7

2.4.1 Local Probing Of a Portion of the Cell 7

2.4.1.1 Atomic Force Microscopy (AFM) 7

2.4.1.2 Young's Modulus Measurement of by AFM 8

2.4.2 Mechanically loading the entire cell 9

2.4.2.1 Micropipette Aspiration 10

2.4.2.2 Micropipette Measurements of RBC Mechanical Properties. 10

2.4.2.2.1 Area Expansion Modulus (K) 11

2.4.2.2.2 Shear Modulus (G) 12

2.4.2.2.3 Bending Modulus (B) 14

2.4.2.3 Microfluidic Devices 15

2.5 Characterization of a Sickle and a Normal Erythrocyte Membrane. 16

2.6 Conditions Affecting Deformability of the RBC Membrane 16

Chapter 3 19

3.0 Computational Modeling 19

3.1 Modeling Procedures using ABAQUS 19

3.1.1 Model Geometry 19

3.1.2 Material Properties 20

3.1.3 Element Selection and Meshing 21

3.1.4 Boundary and loading Conditions 21

3.2 Analytical Modeling using bending Mechanics 23

3.2.1 Assumptions 23

3.2.2 Governing Equations 23

3.2.3 Geometry and cross-section 24

3.3 Analytical Model for Cell Pore Entry 26

3.3.1Assumptions 26

3.3.2 Governing Equations 26

Chapter 4 28

4.0 Results and Discussion 28

4.1 Comparism of Stiffness values between Sickle Erythrocytes 28

4.1.1 Implications of Stiffness and Modulus values obtained from Deformation 30

4.2 Determination of Bending Stresses 31

4.2.1 Implication of Bending stresses and Contour Plots 33

4.3 Effect on Modulus on Cell Aspiration Ratio 34

4.3.1 Estimation of Critical Pressure for Cell Pore Entry 34

4.3.2 Implication of cell response to suction pressure and estimated critical pressures 35

Chapter 5 36

5.0 Conclusion and Recommendation 36

5.1 Conclusion 36

5.1 Recommendations for future work 36

REFRENCE 37

APPENDIX A 42

APPENDIX B 45

LIST OF FIGURES

Figure 2.1: AFM tip on a Sample Surface.[15] 8

Figure 2.2: Force - Indentation Curve, showing hard surface deformation (linear) Cell Surface deformation (Non-Linear)[17]. 9

Figure 2.3: Automated Micropipette[23] 10

Figure 2.4: Schematic Illustrations of Deformation Modes[10] 11

Figure 2.5: Aspirate Distance Equal to Pipette Radius[24] 12

Figure 2.6: Measuring the ratio between Aspirated Length and Radius of the Pipette[24] 13

Figure 2.7: (a-d) Fluidization of a healthy RBC passing through a Microfluidic Channel[36]. 15

Figure 3.1: 3D model of cell 20

Figure 3.2: Boundary and loading conditions on cell 22

Figure 3.3: Deformed and undeformed cell 22

Figure 3.4: beam subjected to pure bending 23

Figure3.5: 2-D geometry of cell 25

Figure 3.6: cross-section of cell 25

Figure 4.1: Force-Displacement curves of oxygenated and ..... deoxygenated sickle cell 28

Figure 4.2: Stress Strain Curve of Oxygenated Sickle cell 29

Figure 4.3: Linear elastic portion of Stress-strain curve for oxygenated sickle cell 30

Figure 4.4: Bending stress distribution 31

Figure 4.5: von Mises stress distribution 32

Figure 4.6: cONTOUR DISTRIBUTION OF VON MISES STRESS 32

Figure 4.8: gRAPH SHOWING aSPIRATION rATIOS OF NORMAL, OXYGENATED AND . DEOXYGENATED SICKLE CELL 34

Figure A.1: Crosssection.....42

Figure A.2: 2D- Geometry.....44

LIST OF TABLES

Table A.1: Bending Stress Values 45

Table B.1: Aspiration ratios for varying suction pressures.....45

CHAPTER 1

1.0 INTRODUCTION

1.1 Background and Motivation

Understanding the mechanisms of any problem affords it a higher probability of being solved. Sickle cell disease being the first molecular disease discovered in 1910 [1] has come a long way in its unraveling, despite this a truly sustainable treatment and management route is still yet to be discovered as cost of management drugs and severity and restrictive nature of bone marrow transplant still have not lowered death tolls due to sickle cell crises[1,2].

Perhaps, our knowledge of the sickling process, undergone by sickle erythrocytes (red blood cells) is not totally representative of its mechanisms and physiological conditions. Currently, the sickling process is seen from a molecular biology point of view [3]with outlined steps from hemoglobin gene mutation to polymerization of sickle hemoglobin (HbS) molecules to vassocultion. Also immense efforts in the field of biomechanics, have explored mechanical properties of diseased and normal erythrocytes [4, 5,6] acknowledging that erythrocytes as well as other living cells can be studied just as other conventional materials.

Despite this, there is a gap in the knowledge of the transition from a biconcave shape to a crescent shape characteristic of irreversibly sickled erythrocytes. Although a few studies

[7] have identified alignment of polymerized sickle hemoglobin (HbS) fibers as possible mechanisms, it still begs the question, why this particular crescent shape and this leads to thoughts that perhaps these fibers do more than just align but may actually contribute to the final shape of the cell by bending the membrane. Hence this work approaches the morphological change noticed in sickling of an erythrocyte from this point of view while acknowledging afore mentioned molecular processes.

1.2 Research Objectives

The general objective of this work is to try to explain to why an erythrocyte with sickle cell properties sickles. This is done using the specific objectives below.

1. To develope a computational model using ABAQUS^{TM} software to induce the sickling of an erythrocyte.
2. To analyze stresses induced along the membrane.
3. To analyze the effect of modulus value on cell entry into pores and estimating critical pressures for cell pore entry.

1.3 Scope of Research

In this work, an erythrocyte with sickle cell properties is modeled as an elastic material with isotropic properties. It is assumed that the cell is at a critical point for morphological change with regards to oxygen tension and sickle hemoglobin concentration (HbS). It is also assumed that polymerization of HbS takes place as cell deformation starts and ends when deformation ends. These assumptions simplify the model and center the focus on testing out the hypothesis. The cell is then subjected to membrane displacements imposed by a 3-point bending configuration.

1.4 Outline of Thesis

This chapter presents a brief background and motivation, as well as the scope and objectives of this research. Chapter 2 embarks on a review of relevant literature beginning from an introduction to erythrocytes and sickle cell disease, common experimental techniques for mechanically characterizing cells and caps up with hemoglobin concentration and oxygen tension effects on erythrocytes with sickle cell trait (SCT). Subsequently, a computational model for inducing sickling of an erythrocyte, analytical model for calculating bending stresses, and determination of critical pressure for cell pore entry is described in chapter 3 before presenting the results in chapter 4. Salient conclusions arising from this work are summarized in chapter 5 along with suggestions for future work.

CHAPTER 2

2.0 LITERATURE REVIEW

2.1 Introduction

Often times, the question why study mechanical properties and their effects on cells, is often asked. But just as mechanical properties of metals, polymers, ceramics and composites, give key insight to their structure-stress relationship, so also, mechanical properties of living cells need to be studied in order to understand their response to stress while in circulation within the body. By doing so, underlying structures of the cells can be deciphered[1].

Furthermore, all cells within the body exist under the influence of specific forces; consequently even a slight disruption of these forces alters the normal functioning of these cells often leading to what is called a diseased state[9].

This chapter begins with an overview of Red blood cells, sickle cell disease, various techniques for deciphering mechanical properties of cells, arguments for fiber alignment as a cause of the final morphology of a sickle cell and ends with a few insights into osmotic pressure, hemoglobin concentration and oxygen tension effects on sickling phenomena.

2.2 The Red Blood Cell (RBC, Erythrocyte)

The red blood cell is one of the four constituents of the blood, With a volume of about 4.5 million cells Per millimeter cube, it earns the title of the largest blood component[10]. They are responsible for transporting oxygen from the lungs to the tissues and carbondioxide from tissue to the lungs[11]. RBC are formed in the bone marrow, live for about 120 days and are destroyed in the spleen. Although the RBC membrane accounts for only 1% of the RBC weight, it plays a very important role in maintaining cell integrity[11].

2.2.1 Function of Erythrocyte membrane

The RBC membrane performs a number of roles namely[11]:

- Assembling and organizing proteins of the lipid bilayer.
- Providing the red cell with its unique deformability and stability.
- Providing a barrier between cytoplasm and the external environment.

The role of RBC membrane in cell deformability and stability would be discussed in more detail in the succeeding section.

2.2.1.1 Deformability of the RBC Membrane

Red cell deformability is very crucial to its survival while in circulation[6]. Deformability is defined as the measure with which the cell is able to undergo large deformations and maintain its normal shape upon unloading without fragmentation or loss of its integrity[11].
Cellular deformability of the RBC membrane depends on three factors:

1. **Cell geometry:** A normal RBC has a characteristic biconcave shape, no subcellular structure such as nucleus and has a hemoglobin solution as its cytoplasm[11]. Because of its unique shape it has less volume for a given surface area, thereby decreasing the bending energy associated with membrane extrusion. The surface to volume ratio (S/V) contribution to cell geometry is very important and a biconcave shape provides a high (S/V) value.

2.**Cytoplasmic Viscosity:** This is determined by the properties and the concentration of the cell hemoglobin[11].

3. **Intrinsic viscoelastic properties of the red cell membrane**

2.3 Sickle Cell Disease

Sickle cell disease is characterized by abnormal rheological properties and a crescent morphology of the red blood cell. It is an inherited disorder that stems from a mutation in the β hemoglobin gene encoding, resulting in the production of sickle hemoglobin molecules (HbS) instead of normal hemoglobin molecules (HbA)[12].

When a sickle cell in its original biconcave shape supplies oxygen to a particular tissue or organ it experiences a state of de-oxygenation, this causes self-assembling of HbS molecules into fibers .

After cycles of sickling and un-sickling, a fraction of the cell becomes irreversibly sickled. This sort of cell exhibits the greatest loss in deformability[13]. While Hemoglobin concentration does not affect the rigidity of normal red blood cells, rigidity of sickle cells is significantly affected by HbS concentration[7, 8].

2.4 Common Experimental Approaches to Mechanical Characterization of Cells

Cells study requires that deformation either by depression or extension of the cell surface is done with a known force or stress while the extent of deformation is being measured [8].

This deformation can be grouped in three namely[9]:

1. Type A: The local probing of only a portion of the cell.
2. Type B: Mechanically loading the entire cell.
3. Type C: The simultaneous loading of population of cells.

Type A and B are discussed in more detail as they concern deformation of a single cell in contrast with Type C method applies more to experiments with the goal of measuring shear flow over a group of cells[9].

2.4.1 Local Probing Of a Portion of the Cell

As the name implies, only a part of the cell is probed for its mechanical properties. Examples of experimental techniques that utilize this principle are Atomic Force Microscopy (AFM) and Magnetic twisting cytometry (MTC). Amongst these two, the AFM technique would be discussed in more detail[9].

2.4.1.1 Atomic Force Microscopy (AFM)

This technique utilizes a tip- scanning approach to image topographies of materials at the atomic or molecular scale[15]. As the tip scans the sample surface through physical contact, the vertical motion of the tip is monitored by photodiodes which detect small changes in the laser beam position reflected from the tip [10]. Nano scale forces are applied to the sample surface through the tip positioned normal to the

free end of a flexible silicon based cantilever displacement which enables mechanical properties of living cells or soft materials can be measured[10], [16].

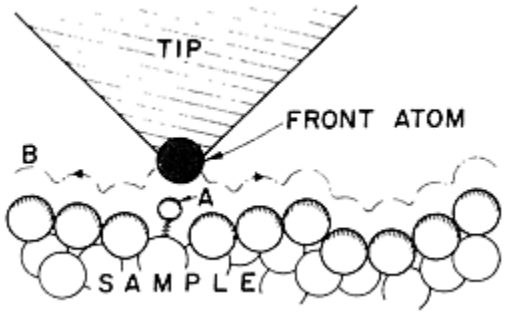

FIGURE 2.1: AFM tip on a Sample Surface.[15]

2.4.1.2 Young's Modulus Measurement of by AFM

The elastic properties of erythrocytes (Red blood cell, RBC) are determined from the force versus distance curve [17] . The extended Hertz model which is a force-extension relationship that is dependent on the tip shape of the AFM indenter is usually employed[18]. For a parabola shaped or spherical tip made of silicon nitride (Si_3N_4), with a curvature radius $R_c$indentation depthΔz , the applied force is related to a relative young's modulus E^* [19] by

$$F = \frac{4\sqrt{R_c}}{3} E^* (\Delta z)^{3/2} \qquad (2.1)$$

For a four sided pyramidal indenter the force as a function of indentation[14] is given by

$$F = \frac{3E\tan\theta}{4(1-\upsilon^2)} \qquad (2.2)$$

The indentation depth of soft samples like RBC, are calculated by subtracting a reference linear force curve of a hard material such as glass or mica from the non-linear force curve of RBC[17].

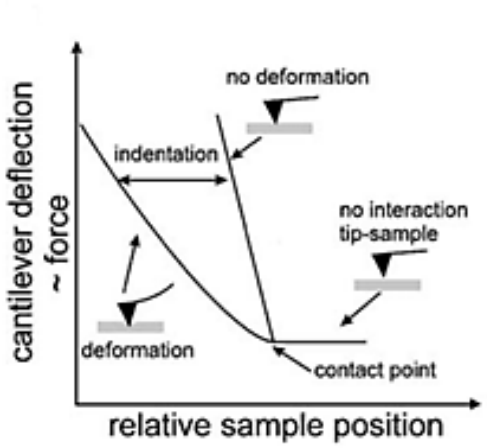

FIGURE 2.2: Force - Indentation Curve, showing hard surface deformation (linear) Cell Surface deformation (Non-Linear)[17].

The relative young's modulus is estimated as a contribution of Young's modulus and Poisson ratios of both AFM tip and sample being studied [20].

$$\frac{1}{E^*} = \frac{1-{\upsilon_1}^2}{E_1} + \frac{1-{\upsilon_2}^2}{E_2} \simeq \frac{1-{\upsilon_1}^2}{E_1} \; for \; E_1 \ll \; E_2 \tag{2.3}$$

Where E_1 and E_2 are sample and AFM tip modulus respectively, and υ_1 and υ_2 are the sample and AFM tip Poisson ratio respectively.

Generally, Young's modulus of living cells range from $1 \sim 100KPa$ [21] and Poisson ratio of living tissues vary between $0.490 \sim 0.499$[22] .

2.4.2 Mechanically loading the entire cell

In this deformation study approach, the entire cell is mechanically loaded to extract its mechanical properties by measuring changes in cell geometry. Examples of experimental techniques that utilize this principle are Micropipette Aspiration (MA) and Optical tweezers [9].

2.4.2.1 Micropipette Aspiration

Micropipette aspiration uses a glass micropipette, with an inner diameter of$1\sim3\ \mu m$, to apply negative pressure onto RBC membranes. When negative pressure is applied, the RBC membrane is aspirated or sucked into the micropipette and the amount of aspiration depends on the viscoelastic properties of cell membrane.

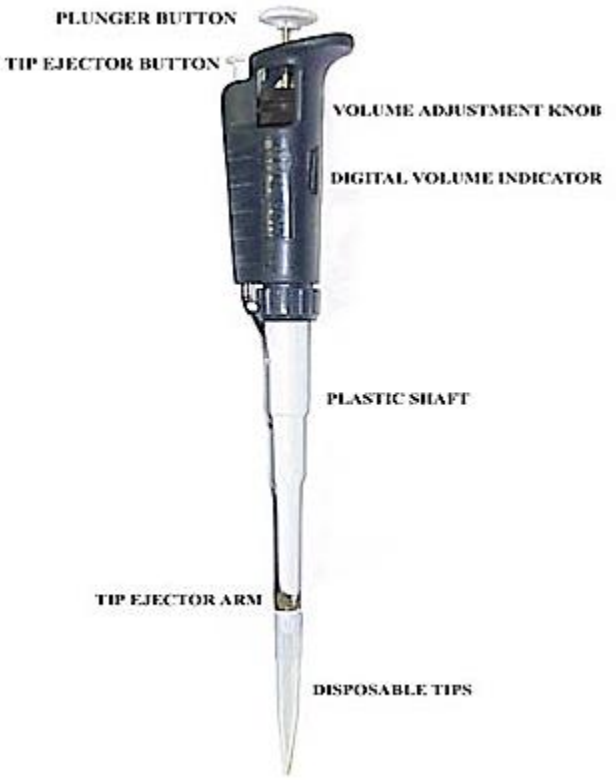

FIGURE 2.3: Automated Micropipette[23]

2.4.2.2 Micropipette Measurements of RBC Mechanical Properties.

Micropipette aspiration (MA)have been used extensively in the measurement of mechanical properties of RBC membrane [1,14,15]. These measurements vary pending on the mechanical

property of interest[10]. Micropipette aspiration has also been used in the study of viscoelastic properties of living cells where time dependent deformation has been observed[16].Depending on the choice of viscoelastic model MA induced deformation can be used to calculate apparent viscosity and relaxation constants of the RBC membrane[16]. RBC membrane deformation can be explained in three modes of deformation namely[10]:

1. Area Expansion or Compression
2. Shear
3. Bending

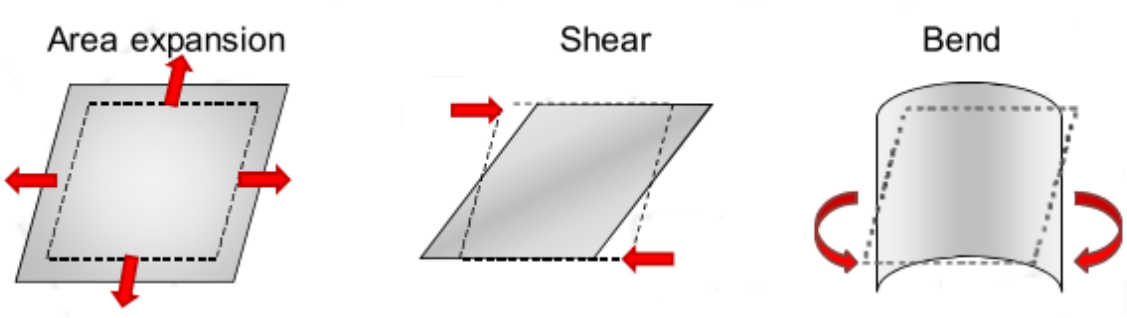

FIGURE 2.4: Schematic Illustrations of Deformation Modes[10]

The membrane modulus value indicates whether or not it is resistant or susceptible to a particular type of deformation.

2.4.2.2.1 Area Expansion Modulus (K)

The Area Expansion Modulus (K) is defined as the elastic energy associated with the isotropic area dilation or compression of a membrane surface[26]. To measure 'K', the micropipette is used

under conditions where the measured aspiration pressure results in an aspiration distance equal to the radius of the pipette[10].

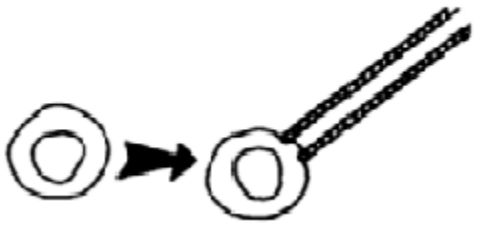

FIGURE 2.5: Aspirate Distance Equal to Pipette Radius[24]

The modulus 'K' is related to an isotropic tensile force and a relative area expansion[26] by:

$$T_t = \frac{K\Delta A}{A_o} \tag{2.4}$$

Where $T_t$is the tensile force, ΔA increase in surface area and A_o is the original surface area.

Experimental based studies report values of 'K' for RBC ranging from $300 - 500\ mN/m$[27].

The area expansion modulus of RBC has been found to be sensitive to temperature [28], with a temperature dependency of $-6mN/m^0C$. At room temperature (25^oC) 'K' for RBC was calculated as $450\ mN/m$[29] .

2.4.2.2.2 Shear Modulus (G)

The Shear modulus 'G' reflects the elastic energy associated with the constant area extension of the membrane surface at an angle 45^o to the direction of extension[10]. To measure 'G', the ratio of aspirated length of membrane to the pipette radius is calculated for a given aspiration pressure [10].

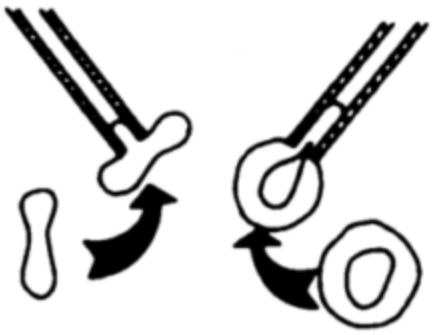

FIGURE 2.6: Measuring the ratio between Aspirated Length and Radius of the Pipette[24]

The modulus 'G' is related to the applied pressure 'P' and pipette radius R_p [17,20]by

$$\frac{\mathrm{D_p}}{\mathrm{R_p}} \sim \frac{\mathrm{PR_p}}{\mathrm{G}} \tag{2.5}$$

Where D_p is the aspirated length of the membrane.

The shear modulus 'G' is also related to a shear force T_s[27] by

$$T_s = \frac{G}{2}(\lambda^2 - \lambda^{-2}) \tag{2.6}$$

Where λ is the extension ratio along the principal axis.

Experimental studies measured 'G' values for RBC ranging from $6 - 10\mu N/m$[14,18, 20, 21].

The influence of temperature on shear modulus [28] is seen in the temperature dependency of $-6 * 10^{-5} mN/m^0C$. At room temperature 'G' for the RBC was calculated as 6.6 $\mu N/m$[29] .

The shear modulus is also influenced by PH values as it was noticed to decrease upon the increase in PH up until 7.2 where the value was constant[31].

2.4.2.2.3 Bending Modulus (B)

The bending or flexural modulus of a membrane is the energy required to deform it from its original curvature to some other curvature[10]. This modulus is responsible for stabilizing the cell shape as they extrude through capillaries or blood vessels[26]. In multi lamellar membrane, bending resistance occurs due to the differential expansion and compression between coupled bilayers or multilayers.

The bending modulus of a two dimensional membrane is related to the bending moment per unit length 'M'[32] by

$$M = B(C_1 + C_2 - C_3) \quad (2.7)$$

Where C_1,C_2 are the principle curvature and $C_3$is the curvature in stress free state.

For a coupled bilayer like RBC the bending modulus is related to the compressibility of the bilayer [33] by

$$B = \frac{h^2 K}{4} \quad (2.8)$$

Where B is the bilayer separation and K is its compressibility.

The RBC membrane 'B' value depends directly on the magnitude of pressure applied when the RBC starts to buckle and inversely on the micropipette area. From experiments done [32] the elastic bending moduli for red blood cell membrane was found to be $10^{-19}Nm \sim 50k_b$T where k_b is the Boltzmann constant and T is absolute temperature .

Also, this value is not significantly affected by temperature [25]or cell hemoglobin concentration[13].

2.4.2.3 Microfluidic Devices

Microfluidic devices are systems that process or manipulate small quantity of fluids using channels with dimensions of $10 - 100\mu m$ [35].This offers new opportunities to control concentration of molecules and cells in space and time. Cell biology is an area of research in which microfluidic systems bring new capabilities[35]. Examples are seen in studies conducted on induced sickling and vassoocclusion of erythrocytes[4, 26].

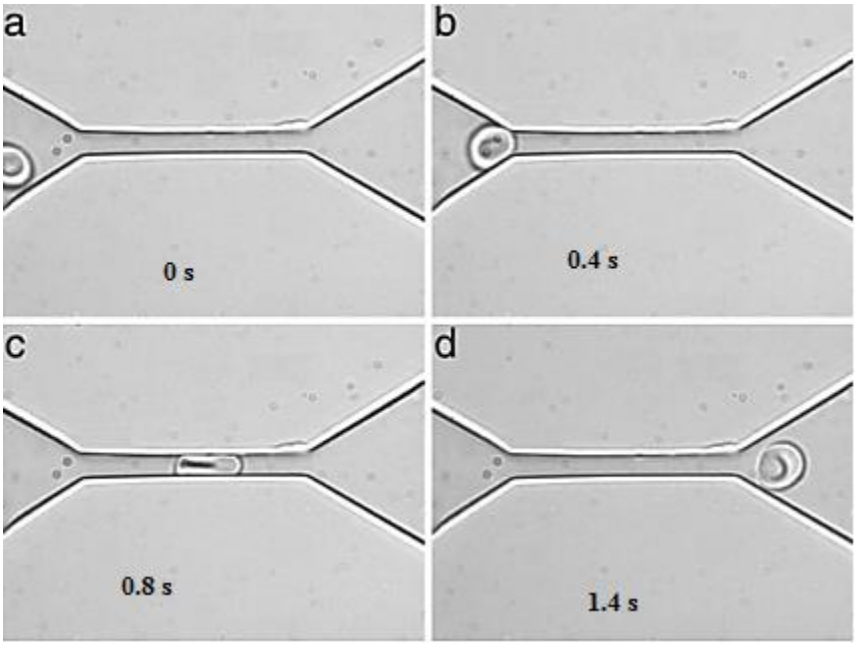

FIGURE 2.7: (a-d) Fluidization of a healthy RBC passing through a Microfluidic Channel[36].

One microfluidic approach developed to study the sickling of red blood cells was done by varying the oxygen partial pressure from 1 kPa to 21 kPa within arrays of micro droplets in flowing oil, to induce depolymerization and polymerization of the hemoglobin, thus providing a method to simulate the cycling that takes place in physiological blood flow[37]. Also, artificial microfluidic environment, were used to induce , control, and inhibit the collective vasoocclusive event in

sickle cell disease by controlling the pressure difference driving the steady flow of blood .They found that sickle hemoglobin polymerization and melting are dependent on oxygen alone and sufficient to recreate jamming and rescue[38].

2.5 Characterization of a Sickle and a Normal Erythrocyte Membrane.

When a sickle cell is in its deoxygenated state the hemoglobin molecules combine to form a long fibrous shape, instead of the normal globular shape[3].The RBC is then transformed into a sickle shape. The sickle-shaped RBC are not able to deform sufficiently to pass through small blood vessels. Thus, the altered shape leads to reduced deformability and obstruction of flow, causing a lack of oxygen supply, vaso-occlusive events and anemia.

The Young's modulus value for oxygenated and deoxygenated sickle cells determined by fitting Eq. (2.1) to the force versus indentation curve were obtained to be $1.0 \pm 1.1KPa$ and $3.30 \pm 2.7KPa$ respectively[39]. Shear modulus for a sickle cell was found to twice that of normal cells[13 , 26]. Thus evidence from these experiments show that the inherited mutations in sickle cell disease are found to markedly reduce the deformability of the RBC.

2.6 Conditions Affecting Deformability of the RBC Membrane

Mechanical properties of the RBC membrane are crucial for optimum deformability of the cell[10]. The following conditions alter these properties and can lead to a diseased state.

Temperature

Studies on effect of temperature on elastic properties of pathophysiological and normal RBC [20, 30]showed that within a temperature range of 2-50 ℃ shear and area compressibility modulus which characterize the surface elastic behavior of the membrane, decreased as temperature increased. In terms of Stiffness, pathophysiological RBC were found to become increasing stiffened as temperature increased when compared to normal RBC[41].

Morphology

Different RBC morphologies exist pending on the diseased condition[5].Higher values of bending and compressibility modulus observed in abnormal RBC suggest a decrease in their deformability[42].

Age of Red Blood Cell

The age of the RBC also affects deformability as surface area and volume of the cell as seen to decrease over the life span of the cell[43].

Osmotic Pressure

Osmotic pressure effects measured in terms of osmolality bring about changes in RBC shape and deformability[10]. At isotonic physiological conditions the RBC maintain their biconcave shape [22].

In hypotonic and hypertonic mediums, the RBC swells due to water intake and shrinks due to water expulsion respectively. During either of these processes the total amount of hemoglobin molecules or mean corpuscular hemoglobin concentration (MCHC) does not significantly change, but its concentration per unit volume changes due to the influx or efflux of water molecules.

Maximum deformability is seen at normal physiological conditions while both hypotonic and hypertonic conditions result in significantly reduced deformability[44].

Mechanical properties of RBC membrane under different osmotic conditions where measured[36,37], in hypotonic conditions, shear and area expansion modulus increased suggesting that non –linear stiffening occurred in the stretched membrane, while under the hypertonic conditions mechanical properties are not significantly changed expect that cytoplasmic viscosity increases.

Hemoglobin Concentration and Oxygen Tension Effect

As already established, in sickle cell disease, intracellular polymerization of hemoglobin occurs upon deoxygenation and leads to a marked increase in intracellular viscosity and elastic stiffness, as well as having indirect effects on the cell membrane. Hemoglobin concentration and oxygen tension effects often occur simultaneously and for cells with mean corpuscle hemoglobin concentration $> 32.1 g/dl$ polymerization occurrs at even oxygen tensions as high as 100mmHg[46] in the very dense cells ($> 45.1 g/dl$).

CHAPTER 3

3.0 Computational Modeling

3.1 Modeling Procedures using ABAQUS

The commercially available ABAQUS^{TM} 6.9 finite element package (Student Edition) is used to induce sickling of an erythrocyte with sickle cell properties. It is assumed that the cell is at a critical point for morphological change with regards to oxygen tension, temperature, PH and sickle hemoglobin concentration (HbS). It is also assumed that polymerization of HbS takes place as cell deformation starts and ends when deformation ends. These assumptions simplify the model and center the focus on testing out the hypothesis, which proposes that HbS fibers impose 3 point bending forces which contribute to the characteristic sickle shape observed during in vivo studies of the sickling processes[30,31].

3.1.1 Model Geometry

A3-D deformable shell continuum, suitable for geometries with one dimension significantly smaller than the others [49] is modeled; while considering continuum membrane mechanics[27] which suggests that red cell molecules are only a few micrometers thick. Cell with diameter of $8\mu m$, outer and inner thickness of $3\mu m$ and $1\mu m$ respectively, are used[11].

Due to symmetry, half of the cell is modeled by revolving the biconcave shape at an angle of 180^{o} along the line of symmetry.

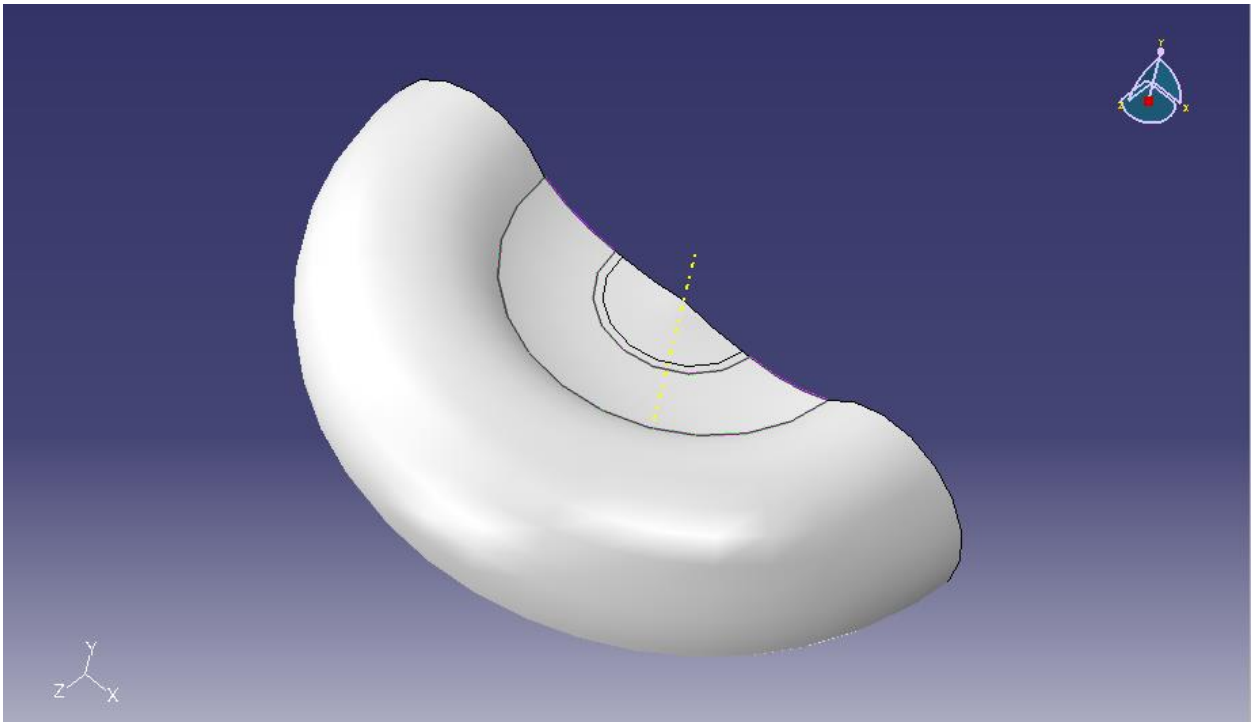

FIGURE 3.1: 3D MODEL OF CELL

3.1.2 Material Properties

The cell is considered as an elastic material capable of large deformation (hyper elastic)[50], and obeys Hookes linear elastic equation.

$$\sigma = \varepsilon E \tag{3.1}$$

Where σ, is the applied stress

E, is the elastic modulus

ε, is the strain induced as a result of the stress

The Young's modulus value of the normal cell, oxygenated sickle cell and deoxygenated sickle cell are approximated from range of values measured in AFM measurements and taken as 0.7KPa, 1.0KPa and 3.0 KPa [39] respectively. Poisson ratio of 0.49[22] was used for all the cell cases.

3.1.3 Element Selection and Meshing

The cell was meshed using linear, finite-membrane-strain, reduced-integration, quadrilateral shell element (S4R) which is robust and suitable for a wide range of applications[49].

3.1.4 Boundary and loading Conditions

The cell was constrained from translating and rotating in the x and y and z axis. At point C shown in Fig 3.2 were allowed boundary displacements in the z-axis as a result of the imposed 3-point bending configuration. The applied load at B ranged from 0 to 400 pN.

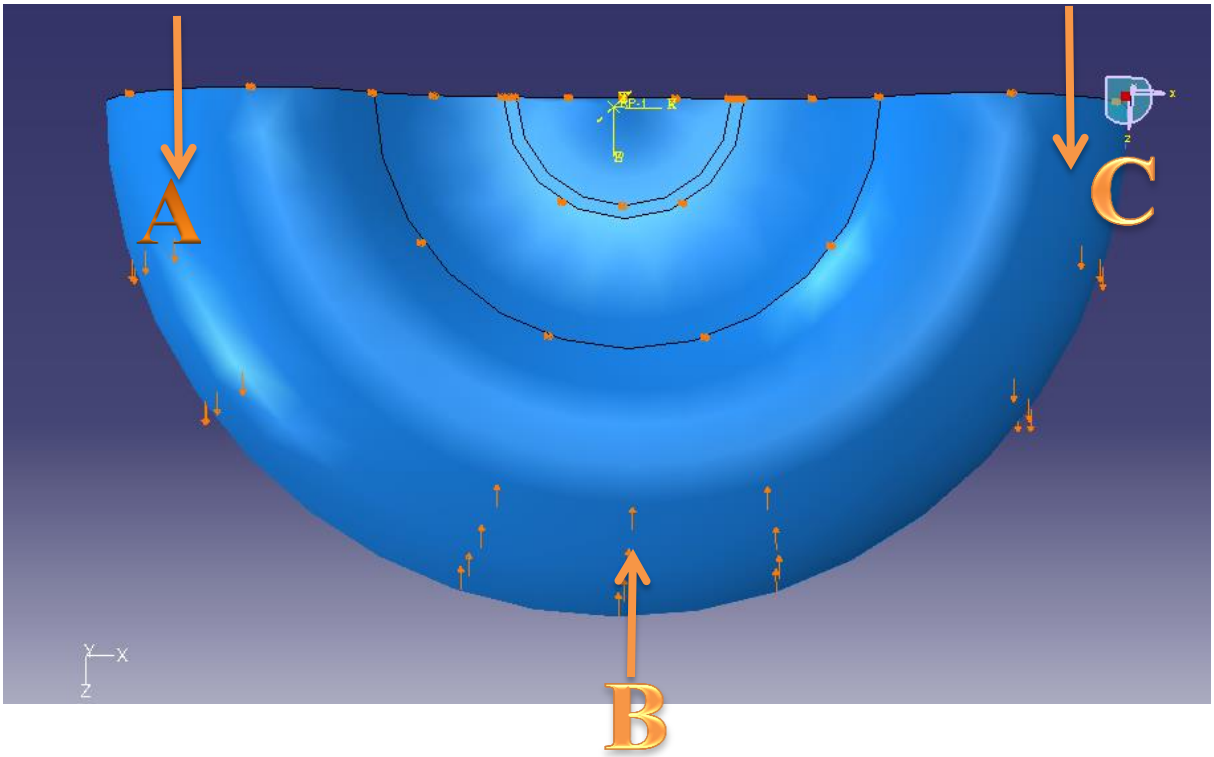

FIGURE 3.2: BOUNDARY AND LOADING CONDITIONS ON CELL

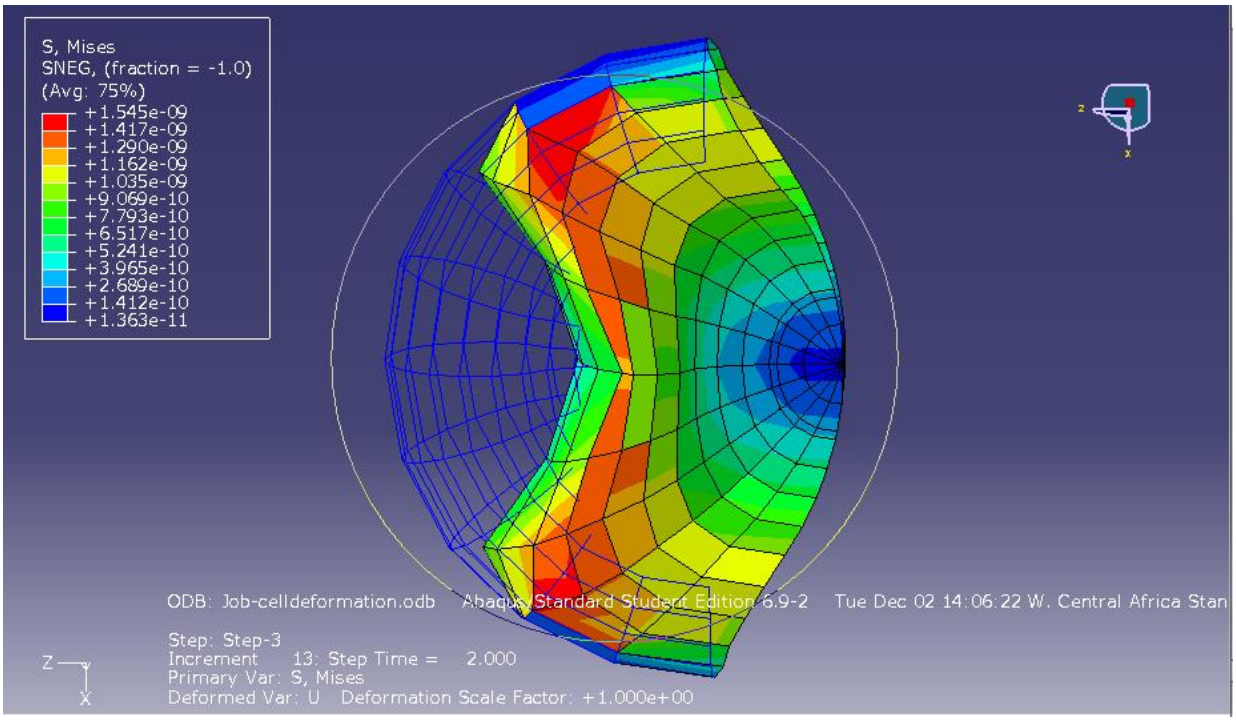

FIGURE 3.3: DEFORMED AND UNDEFORMED CELL

3.2 Analytical Modeling using bending Mechanics

The cell is considered to be under pure bending where the fibers in the cell are considered as straight initially[51]

3.2.1 Assumptions

1. The material of the beam is perfectly homogenous and isotropic
2. The material obeys Hooke's law
3. Transverse sections which where plane before bending remain plane after bending also.
4. Each layer of beam is free to expand or contract independently or the layer above it.
5. Loads are applied in plane of bending

3.2.2 Governing Equations

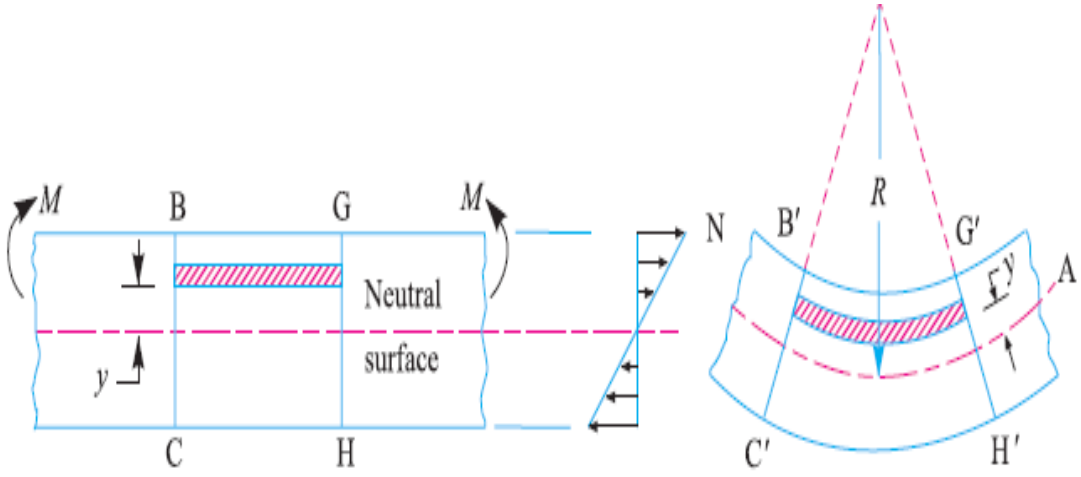

FIGURE 3.4: BEAM SUBJECTED TO PURE BENDING

A beam bent in the configuration shown above is subjected to bending moment, that causes compression in the upper side of the beam, while the lower side becomes extended in tension. A

neutral axis exists between the top and bottom fibers wher the fibers are neither shortened or elongated,this surface is called the neutral axis[52]. The bending equation is given as

$$\frac{M}{I} = \frac{\sigma_b}{y} = \frac{E}{R} \tag{3.2}$$

Where M is the bending moment acting at the given section is given

σ_b is the Bending stress

I is the second moment of area

y is an arbitrary distance from the neutrl axis to the extreme fiber

E is the youngs modulus of the material

R is the radius of courvature.

Since E and R are constant therefore, within the elastic limit, the stress is directly proportional to y[51].

3.2.3 Geometry and cross-section

Just as in the computational modelt he geometry of the cell is considerd as axis symmetric, hence the semi-circular geometry. The centroid y is located at a distance $^{4r}/_{3\pi}$ from the idealized flat top surface.

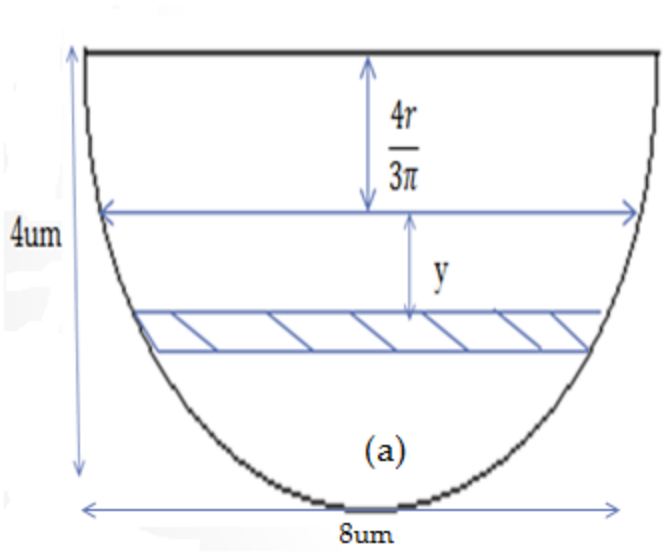

FIGURE3.5: 2-D GEOMETRY OF CELL

Considering the cell to have a biconcave shape an idealized cross section is examined below from the geometry in figure

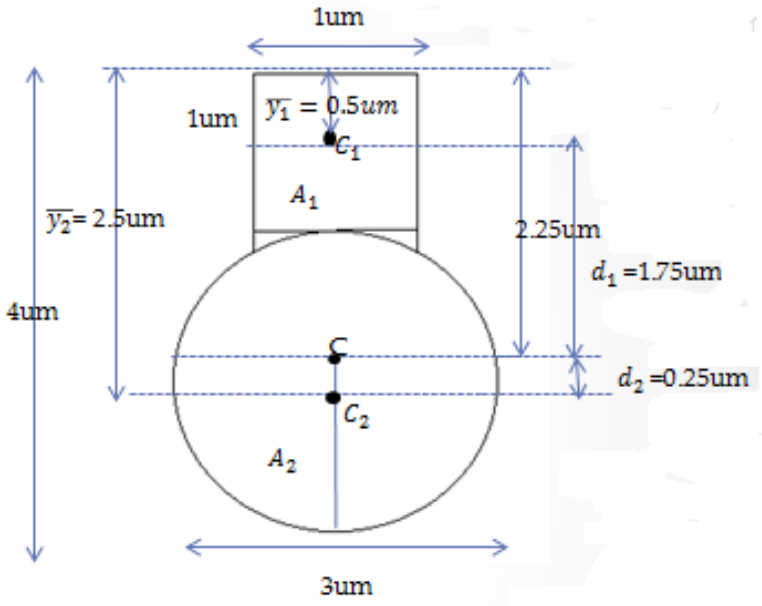

FIGURE 3.6: CROSS-SECTION OF CELL

Deductions and calculation for centroid and second moment of area for this crossection is shown in Appendix A.

3.3 Analytical Model for Cell Pore Entry

The cell pores are considered as micropipette which range from $5{\sim}10um$ for capillaries and $10{\sim}100um$ for arteries [10].

3.3.1Assumptions

1. There is no expansion of the apparent membrane area. This is because there is no excess membrane area.
2. There is no change in volume, since the cytoplasm within the cell is incompressible.

3.3.2 Governing Equations

From the Laplace relationship for a simple spherical drop of fluid case with an internal pressure, and a uniform surface tension [22] the relation[8] below is obtained .

$$\Delta P = 2T_c(\frac{1}{R_p} - \frac{1}{R_c}), \Delta P = P_c \text{ when } \frac{L_p}{R_p} = 1 \quad (3.3)$$

Where ΔP is the suction Pressure

T_c is the cortical or surface tension

R_p is the radius of the micropipette

R_c is the radius of the cell outside the micropipette

P_c is the critical pressure for cell aspiration

L_p is the aspirated length

Using the analysis [53] for an infinite, homogeneous half-space drawn into a micropipette, equation (3.5) is obtained.

$$\frac{\Delta P}{4.39E} = \frac{L_p}{R_p} \tag{3.5}$$

Where

$\frac{2\pi\emptyset}{3} = 4.39$

$\emptyset$ =2.1 is the ratio of micropipette wall thickness to its radius.

For moduli values of 0.7, 1.0 and 3.0 Kpa [39] respectively for normal red blood cell, oxygenated and deoxygenated sickle cell, critical pressures, aspiration ratios for varying suction pressures ranging from 100-3000pN/(um)^2 were estimated.

CHAPTER 4

4.0 Results and Discussion

With the aid of commercially available ABAQUS^{TM} 6.9 finite element software, a sickle cell was deformed in bending and stress distributions obtained. Analytical models were used to estimate bending stresses as well as critical pressure values for normal, oxygenated and deoxygenated sickle cell.

4.1 Comparism of Stiffness values between Sickle Erythrocytes

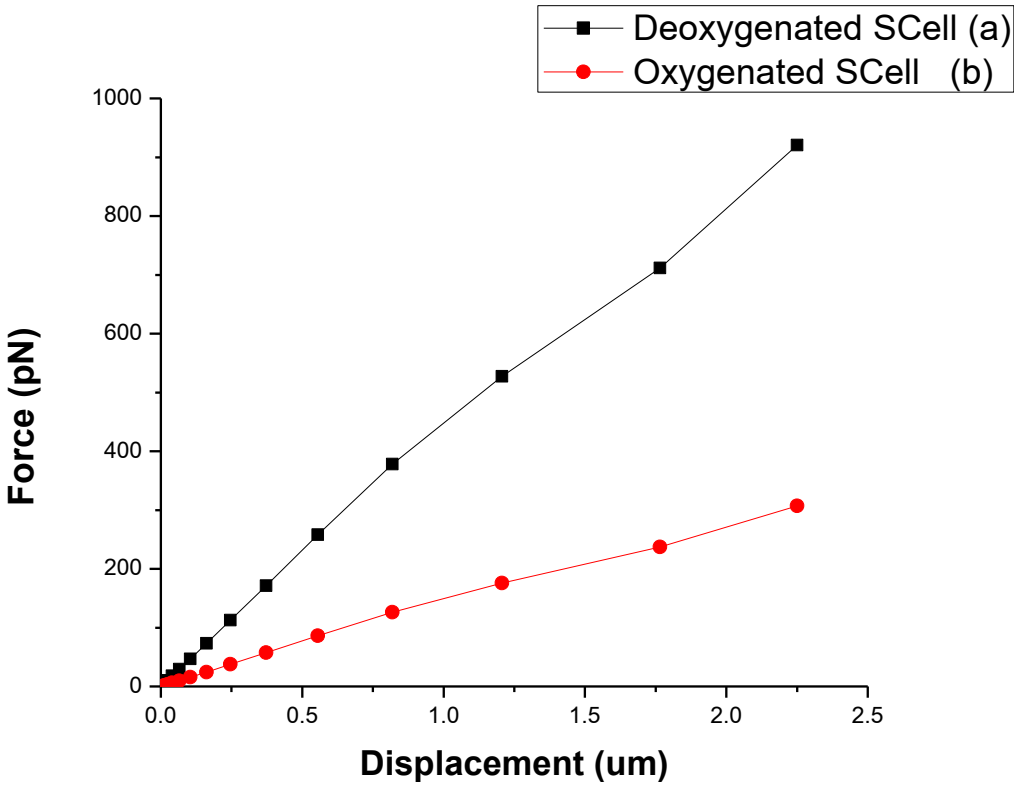

FIGURE 4.1: FORCE-DISPLACEMENT CURVES OF OXYGENATED AND DEOXYGENATED SICKLE CELL

Figure 4.1 compares Force- Displacement curves of oxygenated and deoxygenated sickle cell subjected to the same displacement range. Stiffness values K_a and K_b are calculated for deoxygenated and oxygenated sickle cell respectively using [54]

$$\mathrm{K} = \frac{\Delta \mathrm{F}}{\Delta \mathrm{e}} \tag{4.1}$$

From Hookes law

$$F = Ke \tag{4.2}$$

Where K , is the stiffness

e , is the displacement

Thus values for K_a= 425pN/um and K_b=162pN/um are calculated.

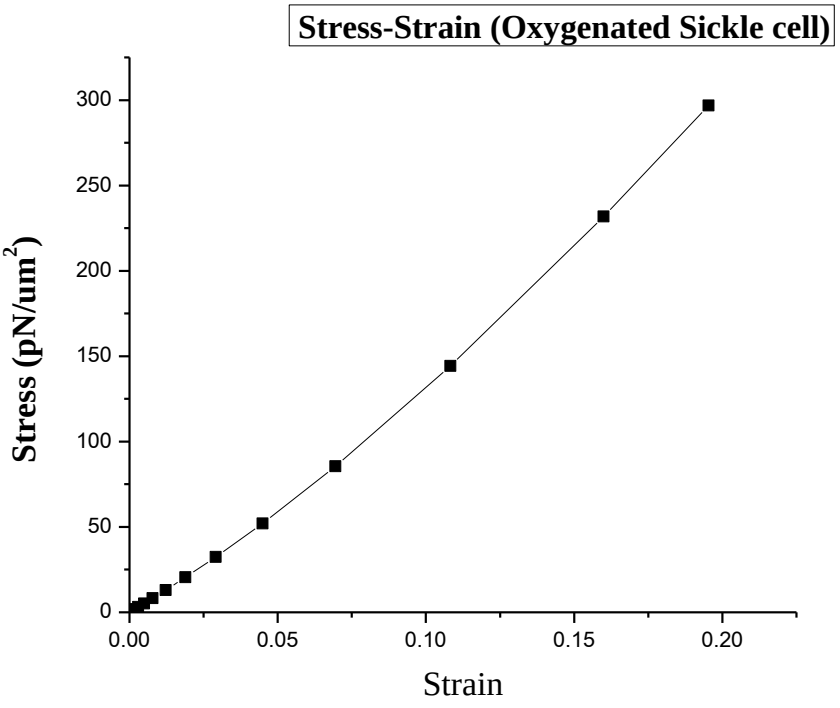

FIGURE 4.2: STRESS STRAIN CURVE OF OXYGENATED SICKLE CELL

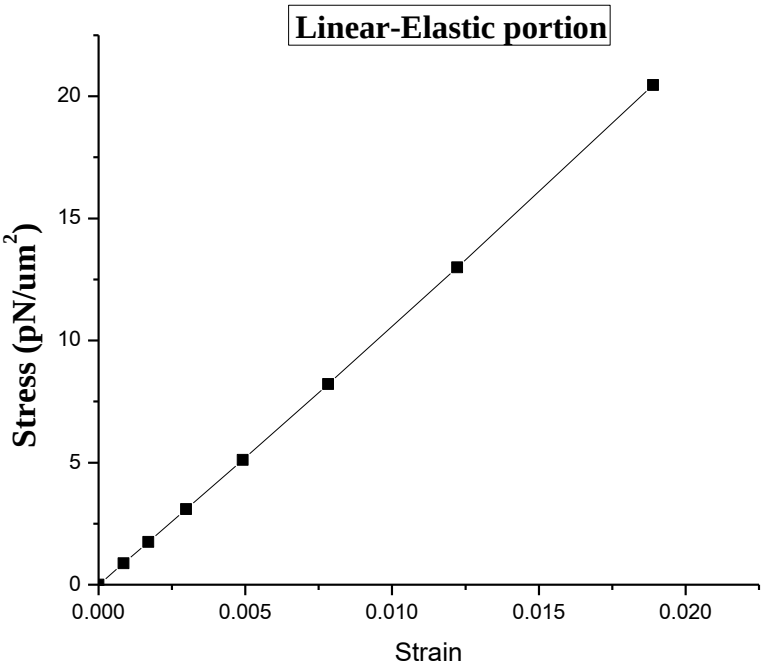

FIGURE 4.3: LINEAR ELASTIC PORTION OF STRESS-STRAIN CURVE FOR OXYGENATED SICKLE CELL

From the linear elastic portion of the stress strain curve in figure 4.2, modulus value of the deformed cell was calculated using $\sigma = E\varepsilon$ [54] and found to be 1.02kPa.

4.1.1 Implications of Stiffness and Modulus values obtained from Deformation

As expected stiffness values increased from a value of K_b=162pN/um to K_a= 425pN/um with an increment of over 100 %. This could be related to stronger bonds [55] being formed within the polymerized cytoplasm as the cell assumes a solid like form when compared to its initial fluid like state with atoms wider apart.

Due to the simplistic nature of the computational model, it could not mirror changes in modulus noticed experimentally when sickling occurs. Nevertheless it provides a basis and direction of thinking for further work.

4.2 Determination of Bending Stresses

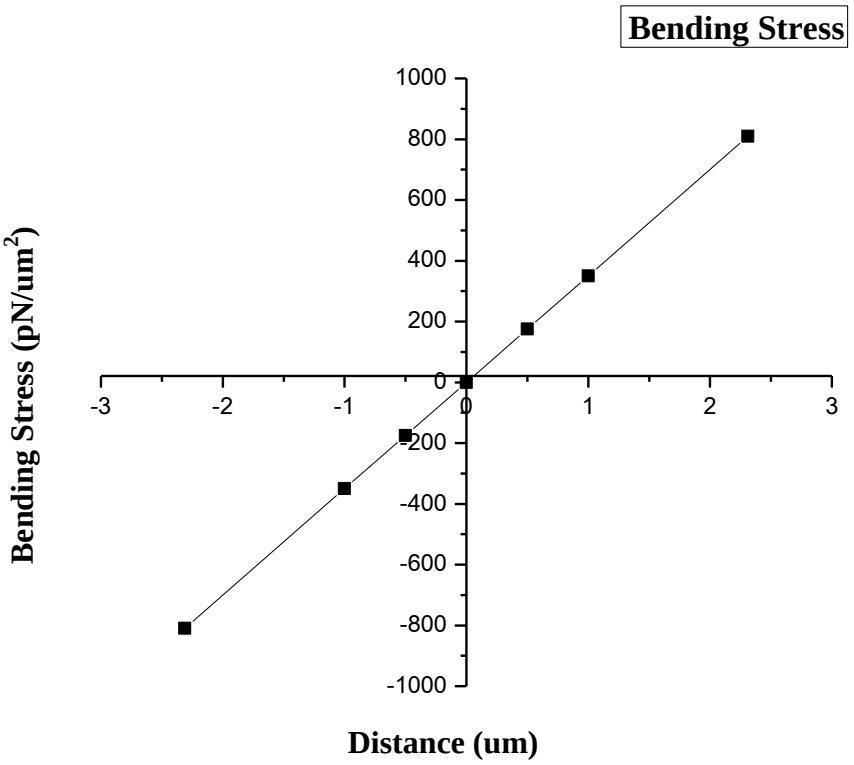

FIGURE 4.4: BENDING STRESS DISTRIBUTION

Figure 4.4 shows bending stress distribution calculated using bending equations stated in equation. A tabular presentation of the obtained bending stresses is shown in appendix A.

Von misses stress values and contours obtained from computational model are shown in figure 4.5 and 4.6 below.

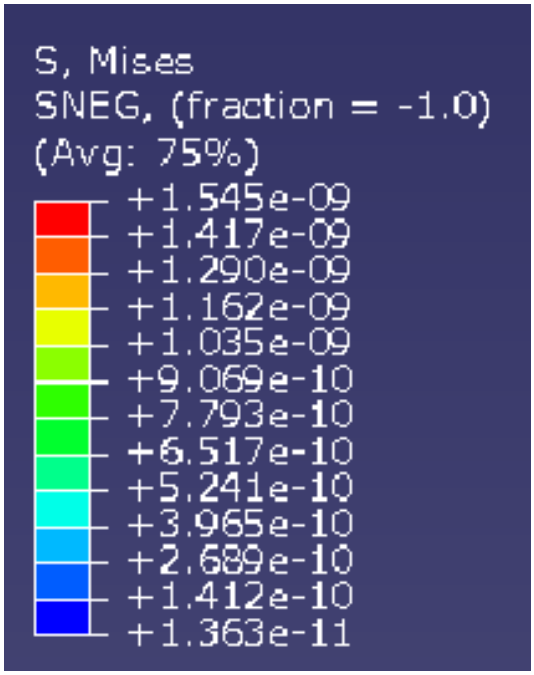

FIGURE 4.5: VON MISES STRESS DISTRIBUTION

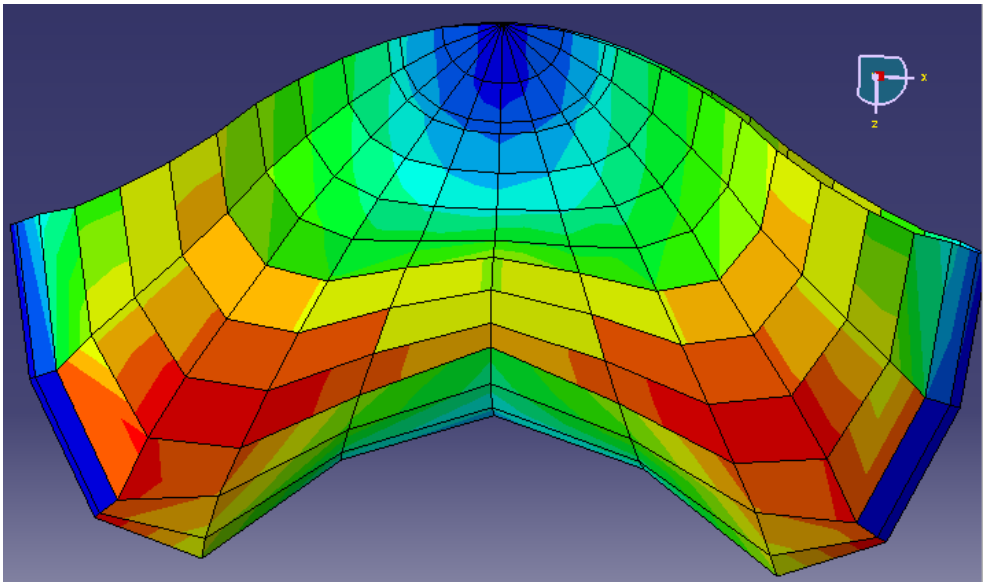

FIGURE 4.6: CONTOUR DISTRIBUTION OF VON MISES STRESS

4.2.1 Implication of Bending stresses and Contour Plots

The stress distribution observed computationally exhibits typical stress distribution contours observed analytically and in theory[51], in that higher bending stresses are experienced at the maximum distance from the centroid or neutral axis.

This goes to show that despite the inability of the computational model to account for moduli changes noticed in practice; it still accurately captures what will happen when a structure is bent.

The maximum bending stress was calculated as $\sigma_{b_{max}} = 7.03 \times \frac{10^{-10}N}{um^2}$, comparing this value to the maximum von mises stress $\sigma_v = 1.59 \times 10^{-9}N/um^2$, it is seen that this does not contradict assumptions made for pure linear elastic bending[51] as this indicates plasticity deformation is yet to begin.

4.3 Effect on Modulus on Cell Aspiration Ratio

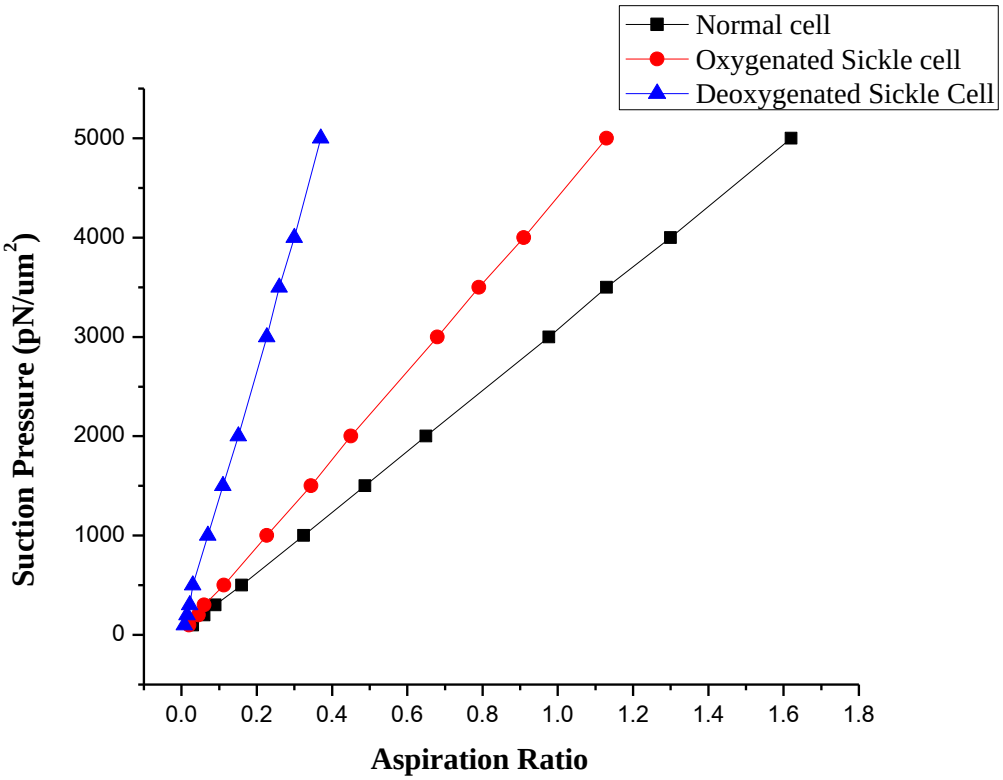

FIGURE 4.8: GRAPH SHOWING ASPIRATION RATIOS OF NORMAL, OXYGENATED AND DEOXYGENATED SICKLE CELL

Aspiration ratio values are calculated using equation (3.4), a tabular representation is presented in Appendix B.

4.3.1 Estimation of Critical Pressure for Cell Pore Entry

Using equation (3.5) critical pressures of for normal, oxygenated and sickle cell are estimated critical pressure values are shown below in table (4.1)

Cell Type	Critical Pressure P_c (N/(um)^2)
Normal Red Blood Cell	3.09 X 10^{-9}
Oxygenated Sickle cell	4.39 X 10^{-9}
Deoxygenated Sickle Cell	1.317X10^{-8}

Table 4.1: Critical pressure values for various cell types

4.3.2 Implication of cell response to suction pressure and estimated critical pressures

Equation (3.5) linearizes the response of the cells to the suction pressure. Comparing aspiration ratios for the three Red blood cells it is seen that the deoxygenated sickle cell is the steepest amongst the three indicating higher stiffness values, and even at suction pressures as high as 5000pN/um^2 , its critical pressure has not been reached. This agrees with experiments which indicate that deoxygenated sickle cells behave like very dense elastic solids [8]and even with suction pressures as high as $350mmHg \sim 4.66 \times 10^{-8} N/um^2$, [56] the cells were not aspirated into micropipettes. In-vivo the body detects this anomalous cells causing and sends signals to the spleen to destroy them. This action most likely leads to anemic condition as the cells are destroyed long before they complete the normal life span of 100 -120 days [48].

CHAPTER 5

5.0 Conclusion and Recommendation

5.1 Conclusion

In this work sickling of an erythrocyte was induced by imposing 3-point bending forces, it was noticed that although the simplistic nature of the model could not mirror change in modulus noticed experimentally, stress distribution observed computationally exhibits typical stress distribution observed analytically and experimentally in bending thus, it provides a basis and direction of thinking for further work and presents bending as a viable explanation to the question, why does an erythrocyte with sickle cell properties assume a crescent shape.

Also, Critical pressure values were estimated for normal, oxygenated and deoxygenated sickle cell, and were found to increase from normal, to oxygenated and then to deoxygenated sickle cell. Aspiration ratio values were found to decrease in the same order.

5.1 Recommendations for future work

1. There is need create a holistic model for sickling of an erythrocyte with sickle cell properties by actually inducing critical conditions so as to mirror modulus change effects noticed in reality.
2. Critical stiffness level for which vassocclusion occurs should be determined taking into orientation and adhesive nature of the cells.

REFRENCE

[1] G. A. Gibson, “Sickle Cell Disease : Still Here and Still Causing Pain A Broader View of the Impact and Needs of SCD.” pp. 1–19, 2011.

[2] S. D. Grosse, I. Odame, H. K. Atrash, D. D. Amendah, F. B. Piel, and T. N. Williams, “Sickle cell disease in Africa: a neglected cause of early childhood mortality.,” *Am. J. Prev. Med.*, vol. 41, no. 6 Suppl 4, pp. S398–405, Dec. 2011.

[3] F. a. Ferrone, “Polymerization and Sickle Cell Disease: A Molecular View,” *Microcirculation*, vol. 11, no. 2, pp. 115–128, Jan. 2004.

[4] H. Byun, T. R. Hillman, J. M. Higgins, M. Diez-Silva, Z. Peng, M. Dao, R. R. Dasari, S. Suresh, and Y. Park, “Optical measurement of biomechanical properties of individual erythrocytes from a sickle cell patient.,” *Acta Biomater.*, vol. 8, no. 11, pp. 4130–8, Nov. 2012.

[5] M. Diez-silva, M. Dao, J. Han, C. Lim, and S. Suresh, “Shape and Biomechanical Human Red Blood Cells in Health,” *MRS Bull.*, vol. 35, no. 5, pp. 382–388, 2010.

[6] N. Mohandas and J. A. Chasis, “Red blood cell deformability, membrane material properties and shape: regulation by transmembrane, skeletal and cytosolic proteins and lipids.,” *Semin. Hematol.*, vol. 30, pp. 171–192, 1993.

[7] H. Lei and G. E. Karniadakis, “Predicting the morphology of sickle red blood cells using coarse-grained models of intracellular aligned hemoglobin polymers.,” *Soft Matter*, vol. 8, no. 16, pp. 4507–4516, Apr. 2012.

[8] R. M. Hochmuth, “Micropipette aspiration of living cells,” *J. Biomech.*, vol. 33, no. 1, pp. 15–22, 2000.

[9] G. Bao and S. Suresh, “Cell and molecular mechanics of biological materials,” *Nat. Mater.*, vol. 2, pp. 715–725, 2003.

[10] Y. Kim, K. Kim, and Y. Park, “Measurement techniques for red blood cell deformability: recent advances,” in *Blood Cell—An Overview of Studies in …*, no. 1, 2012, pp. 168–193.

[11] M. A. Lichtman, T. J. Kipps, U. Seligsohn, K. Kaushansky, and J. . Prchal, *Williams Hematology*, 8th editio. United States: McGraw-Hill, 2010, p. 2460.

[12] G. A. Barabino, M. O. Platt, and D. K. Kaul, “Sickle cell biomechanics.,” *Annu. Rev. Biomed. Eng.*, vol. 12, pp. 345–367, 2010.

[13] E. Evans and N. Mohandas, “Static and Dynamic Rigidities of Normal and Sickle Erythrocytes,” *J. Clin. Invest.*, vol. 73, no. 2, pp. 477–488, 1984.

[14] J. L. Maciaszek and G. Lykotrafitis, “Sickle cell trait human erythrocytes are significantly stiffer than normal,” *J. Biomech.*, vol. 44, no. 4, pp. 657–661, 2011.

[15] G. Binnig and C. . Quate, “Atomic Force Microscope,” *Phys. Rev. Lett.*, vol. 56, no. 9, pp. 930–933, 1986.

[16] K. J. Van Vliet, G. Bao, and S. Suresh, “The biomechanics toolbox : experimental approaches for living cells and biomolecules ☙,” *Acta Biomater.*, vol. 51, pp. 5881–5905, 2003.

[17] M. Targosz, W. Strojny, I. Dulin, and M. Szymon, “Stiffness of normal and pathological erythrocytes studied by means of atomic force microscopy,” *J. Biochem. Biophys. Methods*, vol. 66, no. 1–3, pp. 1–11, 2006.

[18] I. N. Sneddon, “The relation between load and penetration in the axisymmetric boussinesq problem for a punch of arbitrary profile,” *International Journal of Engineering Science*, vol. 3. pp. 47–57, 1965.

[19] A. L. Weisenhorn, M. Khorsandi, S. Kasas, V. Gotzos, and H.-J. Butt, “Deformation and height anomaly of soft surfaces studied with an AFM,” *Nanotechnology*, vol. 4. pp. 106–113, 1999.

[20] M. Radmacher, “Measuringthe Elastic Properties of Biological Samples with the AFM,” *Eng. Med. Biol. Mag.*, vol. 16, no. 2, pp. 47–51, 1997.

[21] M. Radmacher, M. Fritz, C. M. Kacher, J. P. Cleveland, and P. K. Hansma, “Measuring the viscoelastic properties of human platelets with the atomic force microscope,” *Biophysical Journal*, vol. 70. pp. 556–567, 1996.

[22] Y. C. Fung and S. C. Cowin, “Biomechanics: Mechanical Properties of Living Tissues, 2nd ed.,” *Journal of Applied Mechanics*, vol. 61. p. 1007, 1994.

[23] “Micropipette Image.” p. 1, 2011.

[24] E. Evans and P. La Celle, “Intrinsic material properties of the erythrocyte membrane indicated by mechanical analysis of deformation,” *Blood*, vol. 45, no. 1, pp. 29–43, 1975.

[25] T. Shiga, N. Maeda, and K. Kon, “Erythrocyte rheology,” *Critical Reviews in Oncology/Hematology*, vol. 10. pp. 9–48, 1990.

[26] R. Hochmuth and R. Waugh, “Erythrocyte membrane elasticity and viscosity,” *Annu. Rev. Physiol.*, vol. 49, no. 1, pp. 209–219, 1987.

[27] E. A. EVANS, “A NEW MATERIAL CONCEPT FOR THE RED CELL MEMBRANE,” vol. 13, no. 1895, pp. 926–940, 1973.

[28] R. Waugh and E. A. Evans, “Thermoelasticity of red blood cell,” *Biophys. J.*, vol. 26, no. April, pp. 115–131, 1979.

[29] E. A. Evans and R. Waugh, “Osmotic Correction to elastic area compressibility measurements on red cell membrane.,” vol. 20, pp. 307–313, 1977.

[30] S. Chien, K. L. Sung, R. Skalak, S. Usami, and A. Tözeren, “Theoretical and experimental studies on viscoelastic properties of erythrocyte membrane,” *Biophys. J.*, vol. 24, pp. 463–487, 1978.

[31] E. D. Crandall, A. M. Critz, A. S. Osher, D. J. Keljo, and R. E. Forster, “Influence of pH on elastic deformability of the human erythrocyte membrane.,” *Am. J. Physiol.*, vol. 235, pp. C269–C278, 1978.

[32] E. A. Evans, “BENDING ELASTIC MODULUS OF RED BLOOD CELL MEMBRANE DERIVED FROM BUCKLING INSTABILITY IN MICROPIPET ASPIRATION TESTS,” vol. 43, no. July, pp. 27–30, 1983.

[33] E. A. Evans and R. M. Hochmuth, “Mechanochemical properties of membranes,” *Curr. Top. Membr. Transp.*, vol. 10, pp. 1–64, 1978.

[34] G. Nash, C. Johnson, and H. Meiselman, “Influence of oxygen tension on the viscoelastic behavior of red blood cells in sickle cell disease,” *Blood*, vol. 67, no. 1, pp. 110–118, 1986.

[35] G. M. Whitesides, “The origins and the future of microfluidics,” *Nat. Mater.*, vol. 442, pp. 368–373, 2006.

[36] J. Li, G. Lykotrafitis, M. Dao, and S. Suresh, “Cytoskeletal dynamics of human erythrocyte,” vol. 2007, pp. 8–13, 2007.

[37] P. Abbyad, P. Tharaux, J. Martin, N. Baroud, and A. Alexandrou, “Sickling of red blood cells through rapid oxygen exchange in microfluidic drops †,” vol. 10, no. 19, 2010.

[38] J. M. Higgins, D. T. Eddington, S. N. Bhatia, and L. Mahadevan, “Sickle cell vasoocclusion and rescue in a microfluidic device,” 2007.

[39] J. L. Maciaszek, B. Andemariam, and G. Lykotrafitis, “Microelasticity of red blood cells in sickle cell disease,” *J. Strain Anal. Eng. Des.*, vol. 46, no. 5, pp. 368–379, Jun. 2011.

[40] Y. Park and M. Diez-Silva, “Refractive Index maps and membrane dynamics of Human red blood cells parasitized by plasmodiumfalciparum,” *Proc. Natl. Acad. Sci.*, vol. 105, no. 37, pp. 13730–13735, 2008.

[41] M. Marinkovic and M. Diez-Silva, “Febrile Temperature leads to significant stiffening of Plasmodium Falciparum Parasitized erythrocytes.,” *Am. J. Physiol. Cell Physiol.*, vol. 296, no. 1, pp. c59–c64, 2009.

[42] Y. Park, C. A. Best, T. Auth, N. S. Gov, S. A. Safran, and G. Popescu, “Metabolic remodeling of the human red blood cell membrane,” vol. 107, no. 4, pp. 1289–1294, 2010.

[43] B. R. E. Waugh, M. Narla, C. W. Jackson, T. J. Mueller, T. Suzuki, and G. L. Dale, “Rheologic properties of senescent erythrocytes: loss of surface area and volume with red blood cell age,” *Am. Soc. Hematol.*, vol. 79, no. 5, pp. 1351–1358, 1992.

[44] N. Mohandas and M. Clark, “Analysis of factors regulating erythrocyte deformability,” *J. Clin. Invest.*, vol. 66, no. 3, p. 563, 1980.

[45] Y. Tan, D. Sun, S. Member, J. Wang, and W. Huang, “Mechanical Characterization of Human Red Blood Cells Under Different Osmotic Conditions by Robotic Manipulation With Optical Tweezers,” vol. 57, no. 7, pp. 1816–1825, 2010.

[46] C. Dong, R. S. Chadwick, and a N. Schechter, “Influence of sickle hemoglobin polymerization and membrane properties on deformability of sickle erythrocytes in the microcirculation.,” *Biophys. J.*, vol. 63, no. 3, pp. 774–83, Sep. 1992.

[47] D. K. Kaul and M. E. Fabry, “In Vivo Studies of Sickle Red Blood Cells,” *Microcirculation*, vol. 11, no. 2, pp. 153–165, Jan. 2004.

[48] M. H. Steinberg, “Pathophysiology of sickle cell disease,” *Baillieres. Clin. Haematol.*, vol. 11, no. 1, pp. 163–184, 1998.

[49] Dassault system Simulia Corp, “Getting Started with Abaqus: Keywords Edition.” USA, p. 30, 2010.

[50] M. Dao, C. T. Lim, and S. Suresh, “Mechanics of the human red blood cell deformed by optical tweezers,” vol. 51, pp. 2259–2280, 2003.

[51] V. Dias da Silva, *Mechanics and Strength of Materials*. Springer, 1995, p. 531.

[52] “Bending In Straight Beams,” in *Torsional and Bending Stresses in Machine Parts*, pp. 120–180.

[53] D. P. Theret, M. J. Levesque, M. Sato, R. M. Nerem, and L. T. Wheeler, “The application of a homogeneous half-space model in the analysis of endothelial cell micropipette measurements.,” *J. Biomech. Eng.*, vol. 110, pp. 190–199, 1988.

[54] W. D. Callister and J. Wiley, *Materials Science*, 7th ed. John wiley & sons, 2007.

[55] W. Soboyejo, Mechanical Properties of Engineered Materials, 1st ed. New Jersey: Marcel Dekker,Inc, 2003, p. 583.

[56] B. T. Itoh, S. Chien, S. Usarni, I. R. Board, and H. Sciences, “Effects of Hemoglobin Concentration on Deformability of Individual Sickle Cells After Deoxygenation,” pp. 2245–2253, 1995.

APPENDIX A

Determination of centroid position c, and second moment of area $I_{x'x'}$ for the composite crossectional geometry below in figure (A.1)

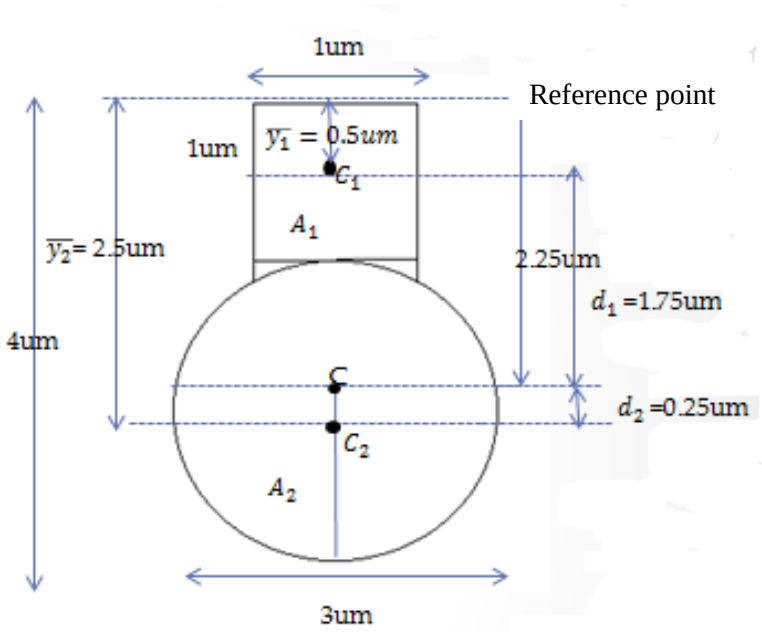

FIGURE A.1: CROSSSECTION

Using parallel axis theorem

$$\bar{y} = \sum_{i=1}^{n} \frac{\bar{y}_i A_i}{A_i} \qquad \text{(A.1)}$$

$$I_{x'x'} = \sum I_{xx} + d^2A \quad \text{(A.2)}$$

Where A_1, is the area of the square cross section

A_2 is the area of the circular cross section

$\overline{y_1}$ and $\overline{y_2}$ are the distance from the reference point to the centroid of respective areas.

c_1 and c_2 are the centroids of A_1 and A_2 respectively

d_1 and d_2 are the distance from the composite centroid c to c_1 and c_2 respectively

I_{xx} for a square cross sectional area $A_1 = \frac{bh^3}{12}$

I_{xx} for a circular cross sectional area $A_2 = \frac{\pi d^4}{64}$

$$\bar{y} = \frac{(0.5 \times 10^{-6}) \times (1 \times 10^{-6})^2 + (2.5 \times 10^{-6} \times \pi \times 1.5^2 \times 10^{-12})}{(1 \times 10^{-12}) + (\pi \times 1.5^2 \times 10^{-12})}$$

$= 2.25um$

$$I_{x'x'} = \frac{(1 \times 10^{-6} \times 10^{-18})}{12} + (1.75 \times 10^{-6})^2 \times (10^{-12}) + \frac{\pi(1.5 \times 10^{-6})^4}{64} + (0.35)^2 \times \pi \times 1.5^2 \times 10^{-12}$$

$= 3.69 \times 10^{-24}\ m^4$

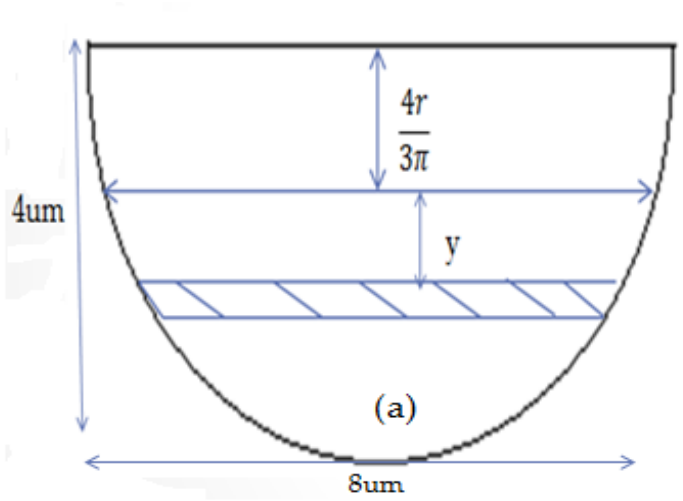

FIGURE A.2: 2D- GEOMETRY

Considering the geometry in figure (A.2)and using the moment relation

$$M = F \times D \tag{A.3}$$

Where F is the perpendicular force (323.61pN) applied at a distance of 4um to the fixed points.

Bending stresses σ_b are calculated for range of $0 \leq y \leq 2.31$ using

$$\sigma_b = \frac{My}{I} \tag{A.4}$$

For $0 \leq y \leq 2.31$

y (um)	**Stress pN/(um)^2**
0	0
0.5	175.1
1.0	350.3
2.31	703.0

TABLE A.1: BENDING STRESS VALUES

APPENDIX B

ΔP pN/um^2	L_p/R_p		
	Normal Cell	Oxygenated Cell	Deoxygenated Cell
100	0.030	0.020	0.007
200	0.060	0.045	0.015
300	0.090	0.060	0.022
500	0.160	0.113	0.030
1000	0.325	0.227	0.070
1500	0.488	0.341	0.110
2000	0.650	0.450	0.151
3000	0.976	0.680	0.227
3500	1.130	0.790	0.260
4000	1.300	0.910	0.300
5000	1.620	1.130	0.370

TABLE B.1: ASPIRATION RATIOS FOR VARYING SUCTION PRESSURES